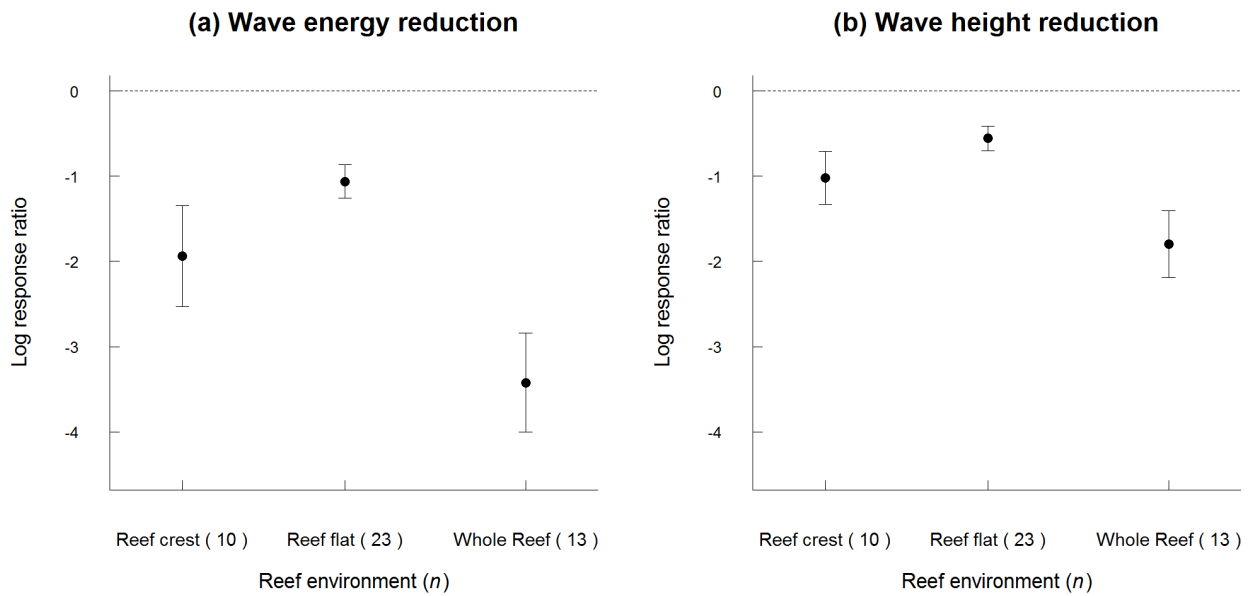
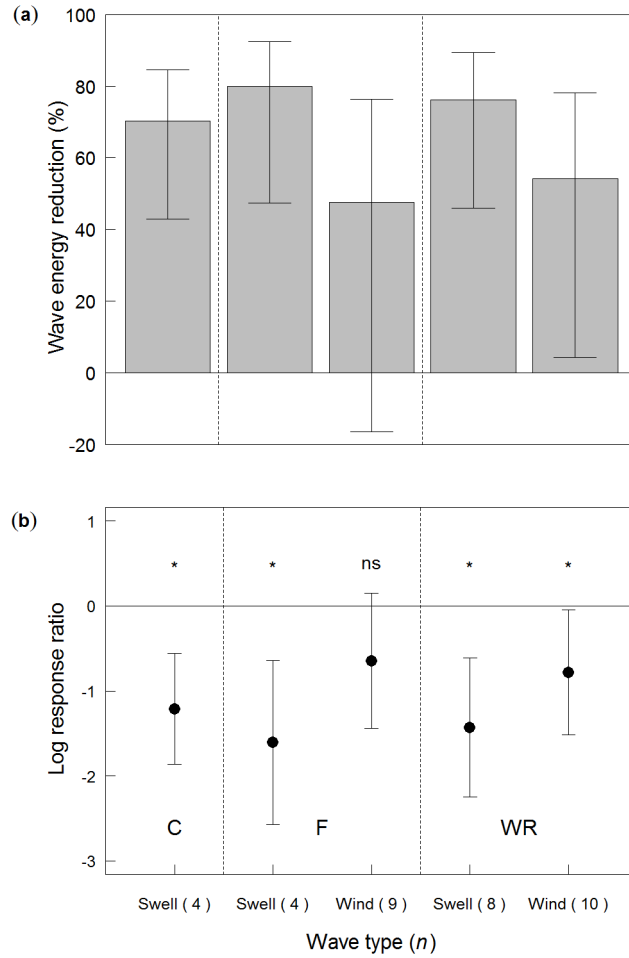


## Supplementary Figures

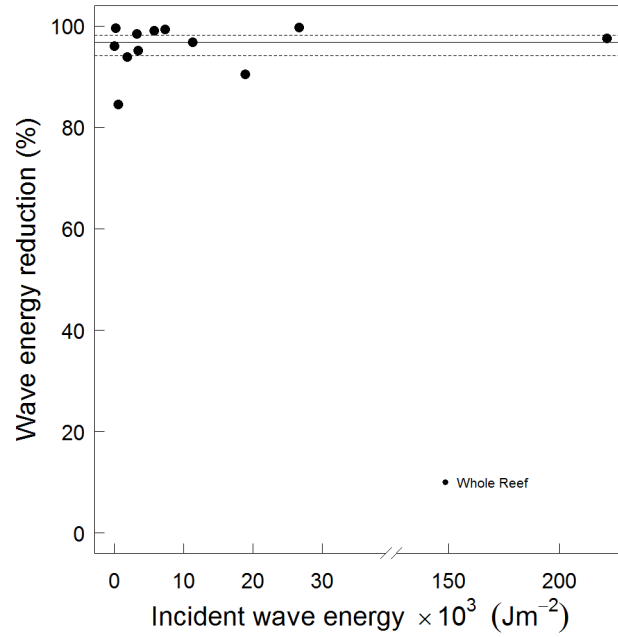


**Supplementary Figure 1. Meta-analysis of the wave attenuation service provided by coral reefs.** Average effect sizes as log response ratios of (a) wave energy reduction and (b) wave height reduction due to each of the reef environments considered. Error bars represent the 95% confidence intervals. When the confidence intervals do not overlap, the averages are considered significantly different from zero ( $P < 0.05$ ). The number of independent experiments analyzed ( $n$ ) is reported in brackets.

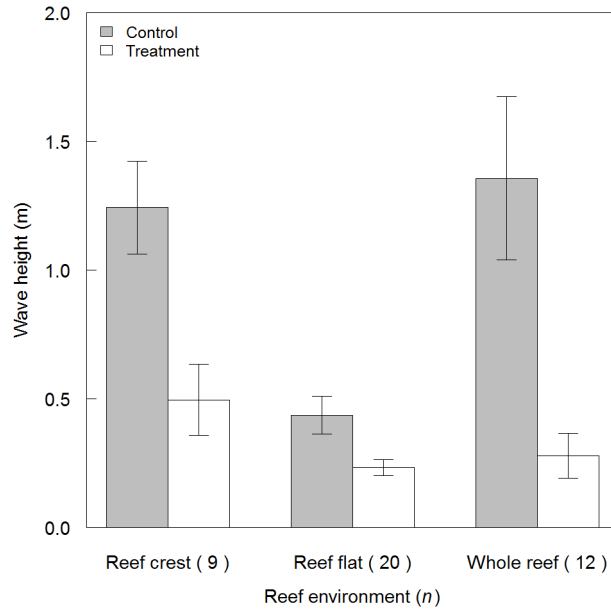


**Supplementary Figure 2. Meta-analyses on wave energy reduction for different wave types.**

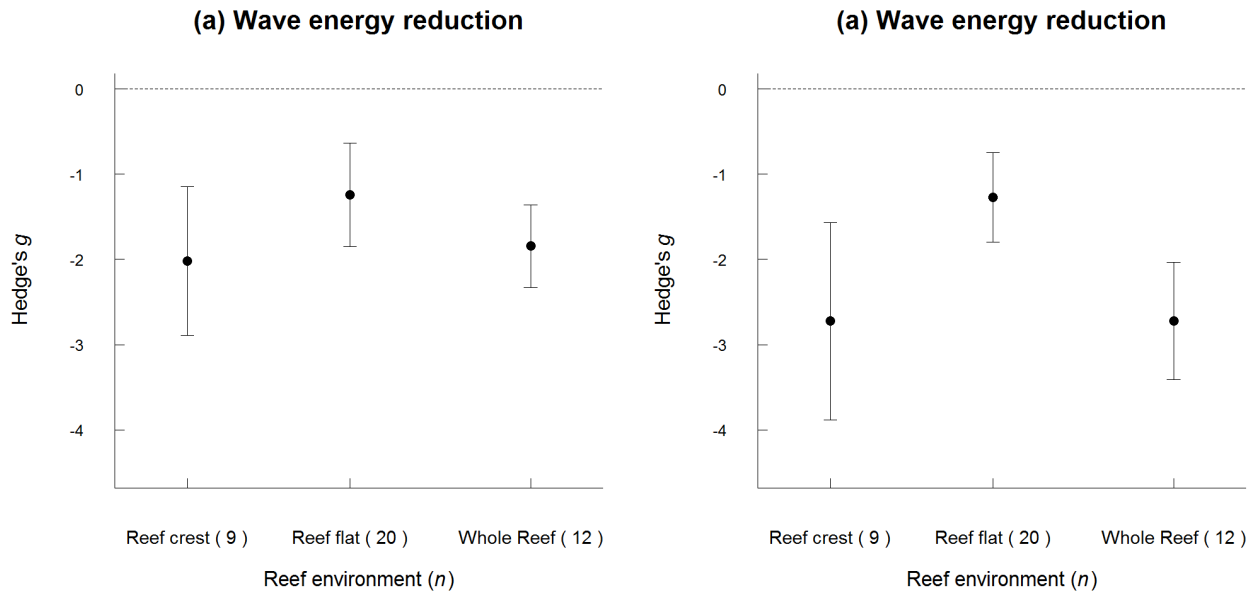
Energy reduction shown as (a) average percentage and (b) average effect sizes calculated as log response ratios. The wave types are: wind waves ( $T = 3-8$  s, “Wind”) and swell ( $T = 8-20$  s, “Swell”). The mean and 95% confidence interval are reported for different reef environments (C= reef crest, F= reef flat, WR= whole reef). When the confidence intervals do not overlap, the averages are considered significantly different from zero. The number of independent experiments ( $n$ ) analyzed is reported in brackets: ns = not significant, \* =  $P < 0.05$ .



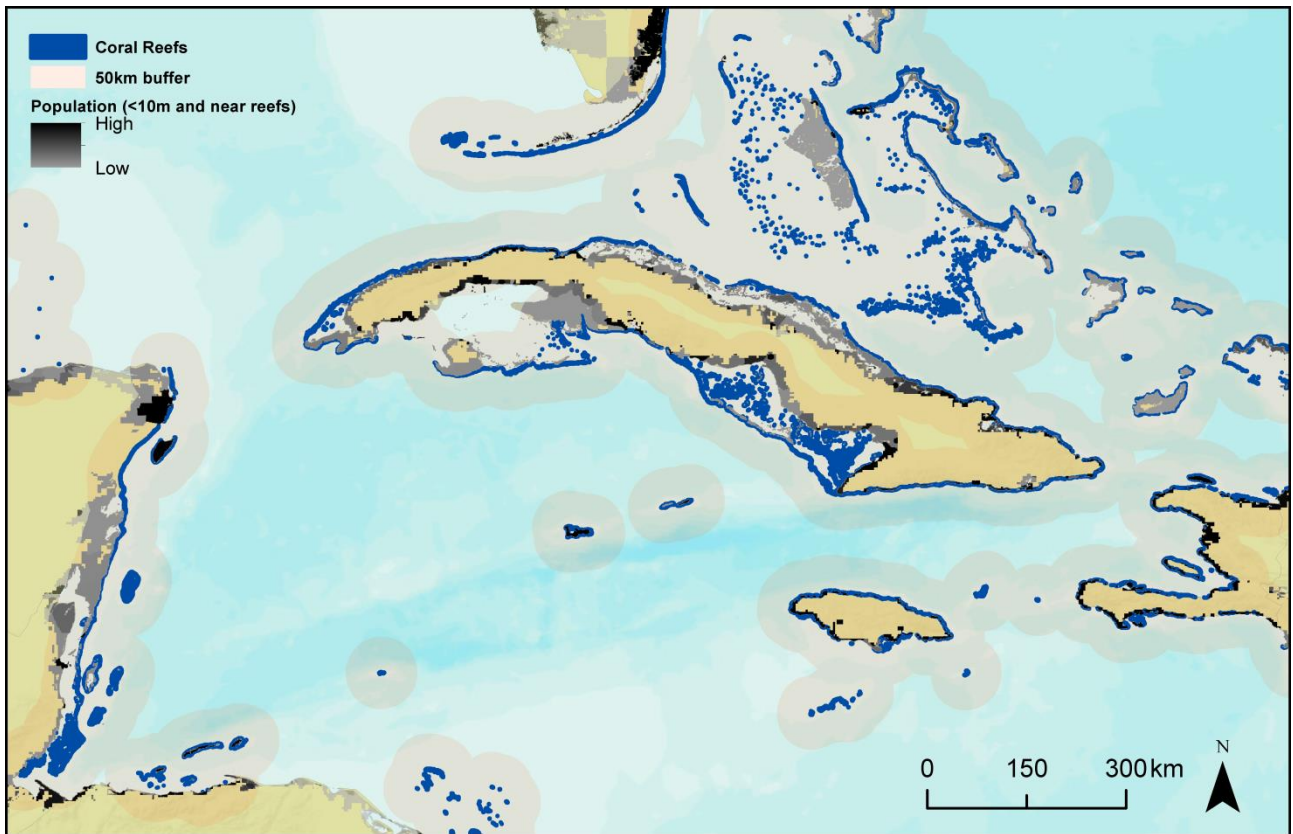
**Supplementary Figure 3. Wave energy reduction as function of maximum energy of incident waves.** Each point represents the percentage of energy reduction computed for individual experiments considering the effect of the whole reef ( $n=12$ ). Wave energy reduction due to the whole reef remains consistent as incident wave energy increases (average = 97% and dashed lines represent 95% confidence intervals from the meta-analysis).



**Supplementary Figure 4. Wave height on coral reef.** Wave height (m) at control (seaward) and treatment (landward) sites for the three coral reef environments considered (C= reef crest, F= reef flat, WR= whole reef). The values are expressed as mean  $\pm$  1 s.e.m. and the number of independent experiments (*n*) analyzed is reported in brackets



**Supplementary Figure 5. Meta-analysis of the wave attenuation service provided by coral reefs.** The average effect size was calculated as Hedge's  $g$  on (a) wave energy reduction and (b) wave height reduction. The average effect size and 95% confidence interval are reported for each coral reef environment considered (C= reef crest, F= reef flat, WR= whole reef). When the confidence intervals do not overlap, the averages are considered significantly different from zero ( $P < 0.05$ ). The number of independent experiments ( $n$ ) analyzed is reported in brackets.



**Supplementary Figure 6. Coral reefs and “at risk” population in the Caribbean.** Detailed view of the Caribbean showing data sets used in our global estimate of the number of people in low-lying areas near reefs. Coral reefs are blue, a 50 km zone around reefs is beige, and the population density (per sq km) ranges from grey (low) to black (high).

## Supplementary Table

**Supplementary Table 1. Studies included in meta-analysis of wave energy dissipation and wave height reduction.** The sample size of both control and treatment for each independent experiment considered belonging to different coral reef environment (C= reef crest; F= reef flat; WR= whole reef) is reported for each reference.

Reference	Reef location	Data <sup>a</sup> Source	Response variables <sup>b, c</sup> ; unit	Sample Size					
				Control			Treatment		
				C	F	WR	C	F	WR
<b>Wave energy dissipation</b>									
1	Kaneohe Bay, Oahu, Hawaii	DER	$E ; J m^{-2}$		3			3	
2	Molokai, Hawaii	DER	$E ; J m^{-2}$			15			15
3	Kaneohe Bay, Oahu, Hawaii	DER	$E ; J m^{-2}$	5	5	5	5	5	5
4	Kaneohe Bay, Oahu, Hawaii	DER	$E ; J m^{-2}$	10			10		
5	Kaneohe Bay, Oahu, Hawaii	DER	$E ; J m^{-2}$	25			25		
6	Hayman Island, Australia (flume model)	DER	$E ; J m^{-2}$			17			17
7	John Brewer Reef, Australia	DER	$E ; J m^{-2}$		10		10		
8	Warraber Island, Australia	DER	$E ; J m^{-2}$		3			3	
9	Australia	SURV	Wave energy dissipation; %	6	6	6	6	6	6
10	Lady Elliot Island, Australia	DER	$E ; J m^{-2}$		3			3	
11	Warraber Island, Australia	DER	$E ; J m^{-2}$		57			39	
12	Sandy Bay, Ningaloo Reef, Australia	DER	$E ; J m^{-2}$	15			15		
13	Ipan Reef, Guam	DER	$E ; J m^{-2}$	50	50	50	50	50	50
14	Great Pond Bay, St. Croix, US Virgin Island	DER	$E ; J m^{-2}$	8	8	8	8	8	8
15	Tague Reef, St. Croix, US Virgin Island	DER	$E ; J m^{-2}$	110			110		
16	Hulhudhoo Reef, South Maalhosmadulu atoll, Maldives (North West, North East, South West, South East)	DER	$E ; J m^{-2}$		5			5	
					5			5	
					5			5	
					5			5	

17	Minatogawa fishery port, Japan (flume model)	DER	$E ; J m^{-2}$			3			3
18	Yongshu Reef, Nansha Islands, China	SURV	Wave energy dissipation; %		18			18	
19	Puerto Morelos, Mexico	DER	$E ; J m^{-2}$			75			75
20	Sandy Bay, Ningaloo Reef, Australia	DER	$E ; J m^{-2}$	10	10	10	10	10	10
21	Derawan Island, Indonesia	DER	$E ; J m^{-2}$	195			195		
22	Majuro Atoll, Marshall Islands	DER	$E ; J m^{-2}$	20			20		
23	Lady Elliot Island, Australia	DER	$E ; J m^{-2}$			15			15
24	Mtsanga Gouela beach, Mayotte Dapani beach, Mayotte Trevani beach, Mayotte	DER	$E ; J m^{-2}$	5			5		5
						5			5
25	Kandumeygalaa, Huvadho, Maldives Dhakandho, South Maalhosmadulu, Maldives	DER	$E ; J m^{-2}$	5			5		
				5			5		
26	Mokuleia, Oahu, Hawaii	DER	$E ; J m^{-2}$	192	192	192	192	192	192
27	Red Beach, Whangaparaoa Peninsula, New Zealand	DER	$E ; J m^{-2}$	21			6		
<b>Wave height reduction</b>									
1	Kaneohe Bay, Oahu, Hawaii	SURV	$H_s ; m$			3			3
2	Molokai, Hawaii	SURV	$H_s ; m$				15		15
3	Kaneohe Bay, Oahu, Hawaii	SURV	$H_{rms} ; m$	5	5	5	5	5	5
4	Kaneohe Bay, Oahu, Hawaii	SURV	$H_{rms} ; m$	10			10		
5	Kaneohe Bay, Oahu, Hawaii	SURV	$H_{rms} ; m$	25			25		
6	Hayman Island, Australia (flume model)	EXP	$H ; m$				17		17
7	John Brewer Reef, Australia	SURV	$H_s ; m$		10		10		
8	Warraber Island, Australia	SURV	$H_s ; m$		3			3	
9	Australia	SURV	Wave height dissipation; %	6	6	6	6	6	6
10	Lady Elliot Island, Australia	SURV	$H_s ; m$		3			3	
11	Warraber Island, Australia	SURV	$H_{m0} ; m$		57			39	
12	Sandy Bay, Ningaloo Reef, Australia	SURV	$H_s ; m$	15			15		
13	Ipan Reef, Guam	SURV	$H_s ; m$	50	50	50	50	50	50
14	Great Pond Bay, St. Croix, US Virgin Island	SURV	Significant wave height; m	8	8	8	8	8	8



15	Tague Reef, St. Croix, US Virgin Island	SURV	Significant wave height; m	110			110		
16	Hulhudhoo Reef, South Maalhosmadulu atoll, Maldives (North West, North East, South West, South East)	SURV	$H_s$ ; m		5			5	
					5			5	
					5			5	
17	Minatoga fishery port, Japan (flume model)	EXP	$H_s$ ; m			3			3
18	Yongshu Reef, Nansha Islands, China	SURV	Wave height dissipation; %		18			18	
					85			85	
19	Puerto Morelos, Mexico	SURV	$H_s$ ; m			75			75
20	Sandy Bay, Ningaloo Reef, Australia	SURV	$H_{rms}$ ; m	10	10	10	10	10	10
21	Derawan Island, Indonesia	SURV	$H_s$ ; m	195			195		
22	Majuro Atoll, Marshall Islands	SURV	$H_s$ ; m	20			20		
23	Lady Elliot Island, Australia	SURV	$H_s$ ; m			15			15
24	Mtsanga Gouela beach, Mayotte	SURV	$H_s$ ; m	5			5		
	Dapani beach, Mayotte					5			5
	Trevani beach, Mayotte					5			5
25	Kandumeygalaa, Huvadhoo, Maldives	SURV	$H_s$ ; m	5			5		
	Dhakandhoo, South Maalhosmadulu, Maldives			5			5		
26	Mokuleia, Oahu, Hawaii	SURV	$H_s$ ; m	192	192	192	192	192	192
27	Red Beach, Whangaparaoa Peninsula, New Zealand	SURV	$H_{m0}$ ; m	21			6		

(a) Data Source indicates if data were collected during a survey in the field (SURV), resulted from experimental activity (EXP), or derived from other original measures (DER)

(b) The response variable, wave height, is reported as cited in the original study.  $H_s$ = significant wave height;  $H_{rms}$  = root-mean-square wave height;  $H_{m0}$ = significant wave height. Wave height data were transformed to  $H_{1/3}$ .

(c)  $E$  is wave energy density calculated from  $H_{1/3}$  using equation (1)

**Supplementary Table 2. Range of incident wave heights for experiments used to investigate the wave energy reduction as function of maximum energy of incident waves.** The range of wave heights at control site (i.e., the incident waves) for each independent experiment considered belonging to different coral reef environment (i.e., reef flat, reef crest, whole reef) is reported for each reference. The control site for reef crest and whole reef is the fore reef; the control site for reef flat is the most seaward sensor on the reef flat. For experiments where data were available for both the reef crest and whole reef environments, the control site was the same.

Reference	Reef location	Region	Wave height range (m) minimum–maximum		
			Reef Flat	Reef Crest	Whole Reef
<sup>20</sup>	Sandy Bay, Ningaloo Reef	Australia	0.12 - 0.50	0.50- 2.14	0.50 - 2.14
<sup>7</sup>	John Brewer Reef	Australia	0.24 - 0.78		
<sup>10</sup>	Lady Elliot Island	Australia	0.20 - 0.36		
<sup>12</sup>	Sandy Bay, Ningaloo Reef	Australia		0.55 - 2.02	
<sup>8</sup>	Warraber Island	Australia	0.31 - 0.50		
<sup>6</sup>	Flume (model of Hayman Island)	Australia			1.00 - 3.88
<sup>23</sup>	Lady Elliot Island	Australia			0.69 - 2.42
<sup>13</sup>	Ipan Reef	Guam	0.04 - 0.79	0.62 - 4.61	0.62 - 4.61
<sup>1</sup>	Kaneohe Bay, Oahu	Hawaii	0.32 - 0.57		
<sup>3</sup>	Kaneohe Bay, Oahu	Hawaii	0.42 - 0.57	1.29 - 1.61	1.29 - 1.61
<sup>5</sup>	Kaneohe Bay, Oahu	Hawaii		1.10 - 3.18	
<sup>4</sup>	Kaneohe Bay, Oahu	Hawaii		1.47 - 3.51	
<sup>2</sup>	Molokai	Hawaii			0.13 - 0.44
<sup>26</sup>	Mokuleia, Oahu	Hawaii	0.58 - 2.43	0.64 – 3.00	0.64 – 3.00
<sup>17</sup>	Flume (model of Minatogawa fishery port)	Japan			0.04 - 0.12
<sup>16</sup>	Hulhudhoo Reef, South Maalhosmadulu atoll	Maldives	0.15 - 0.21		
<sup>16</sup>	Hulhudhoo Reef, South Maalhosmadulu atoll	Maldives	0.16 - 0.30		
<sup>16</sup>	Hulhudhoo Reef, South Maalhosmadulu atoll	Maldives	0.06 - 0.09		

<sup>16</sup>	Hulhudhoo Reef, South Maalhosmadulu atoll	Maldives	0.06 - 0.08		
<sup>25</sup>	Dhakandhoo, South Maalhosmadulu	Maldives	0.18 - 0.44		
<sup>25</sup>	Kandumeygalaa, Huvadhoo	Maldives	0.12 - 0.22		
<sup>22</sup>	Majuro Atoll	Marshall Island	0.28 - 0.77		
<sup>24</sup>	Mtsanga Gouela beach	Mayotte	0.61 - 1.00		
<sup>24</sup>	Dapani beach	Mayotte			0.32 - 1.21
<sup>24</sup>	Trevani beach	Mayotte			0.32 - 1.65
<sup>19</sup>	Puerto Morelos	Mexico			0.53 - 13.26
<sup>15</sup>	Tague Reef, St. Croix	US Virgin Is.		0.25 - 0.27	
<sup>14</sup>	Great Pond Bay, St. Croix	US Virgin Is.	0.17 - 0.47	0.46 - 0.66	0.46 - 0.66

## Supplementary Methods

**Screening protocol to identify relevant articles.** We adopted a screening protocol based on two selection criteria to identify relevant articles<sup>28</sup>. First, we first evaluated abstracts to exclude languages other than English, publication of abstract only, and articles clearly not focused on wave attenuation. Then we reviewed the full text of publications that passed the first screening and selected only publications reporting original data acquired from either lab experiments or field surveys. We considered modeling studies only when they had original data that was used for model validation.

We identified 255 relevant articles on coral reefs and wave attenuation from the literature search and identified six additional references from article citations and previous preliminary article searches.

**Reef and wave characteristics of considered studies.** The median width of reef flats analyzed was 184 m and ranged between 34 m and 3200 m; the majority of the reef flats were 34 m to 300 m wide. For the studies included in our analysis, waves approaching reefs had an average height of  $1.4 \text{ m} \pm 0.3 \text{ m s.e.m.}$ , while those propagating from the reef crest to the shoreline were on average  $0.4 \text{ m} \pm 0.1 \text{ m s.e.m.}$  high (Supplementary Fig. 4).

**Wave attenuation measure.** Wave energy reduction is defined as the loss in wave energy density that occurs as the waves interact with the reef during their propagation towards shore. Wave height reduction occurs when waves interact with the reef. An oceanic surface gravity wave begins to interact with the sea floor when the water depth is equal to half the wavelength ( $d = \lambda/2$ ). Along a cross-shore transect on a typical coral reef, water depth decreases rapidly on the fore reef up to the reef crest and it remains shallow on the reef flat (Fig. 1). Incident wave heights approaching the reef

can increase locally due to wave energy convergence from refraction and/or shoaling<sup>29, 30</sup>, but then generally rapidly decrease at the reef crest due to depth-induced breaking. Wave heights are typically depth-limited on the relatively shallow reef flat<sup>7</sup>.

**Data extraction.** For each variable, we extracted the mean, error of the mean (standard deviation or standard error), and sample size. If the error of the mean or the sample size was not clearly reported and a minimum of 3 replicate values were available, we pooled the data to calculate a new mean value, its associated error, and sample size. In one case, where authors reported mean, sample size, and the range, we estimated standard deviations using the methodology described by Hozo *et al.*<sup>31</sup>.

For most of the papers, we had to extract data from time series plots of wave height to calculate the relevant statistics. Where the data were depicted on the plot with a symbol and referred to a specific time point, we collected all of the data in the series. Otherwise, if only the wave height trend was shown and no specific symbols were drawn, we sampled the time series with an effort proportional to the series length. We extracted 5 random points for series from 0 to 14 days, increasing 5 units every other 14 days (e.g.,  $n=5$  for 14 days,  $n=10$  for 28 days). We sampled the same time points along the time series for both control and treatment groups.

We did not specifically consider water depth as a factor in our analyses, since specific tidal elevation data were not available for all the locations where waves were measured along the transects. However, relevant statistics used in meta-analyses were computed by pooling wave data extracted at different stages of the tidal cycle. For example, time series length was comprehensive of cyclic variation in water levels due to tides. Our analyses, therefore, and in particular the meta-analyses, examined the full tidal range. Because wave height was reported in different studies with different notations (namely, ' $H_s$ ', 'Significant wave height', ' $H_{mo}$ ', or ' $H_{rms}$ '), we transformed all heights in the common metric  $H_{1/2}$ . In particular, following Holthuijsen<sup>32</sup>, we considered notations

‘ $H_s$ ’, ‘ $H_{mo}$ ’, and the more generic term ‘Significant wave height’, equivalent for  $H_{1/3}$  while we transformed ‘ $H_{rms}$ ’ in  $H_{1/3}$  using the inverse of the equation

$$H_{rms} = 1/2 \times \sqrt{2} \times H_{1/3}. \quad (1)$$

Using supplementary equation (1), we transformed wave height data extracted for wave height reduction into energy data to increase the sample size of related wave energy reduction studies.

When reported, we extracted the specific distance between wave sensors.

When possible, we extracted data about specific wave type. We considered three wave types: wind waves (wave period,  $T = 3-8$  s), swell waves ( $T = 8-20$  s), and infragravity waves ( $T > 20$  s).

Wind and swell waves are both gravity waves generated by wind friction on the sea surface<sup>32</sup>.

Infragravity waves are primarily generated by nonlinear-wave interactions along the coastline<sup>33, 34</sup>.

It was not possible to identify and separate wave frequency in each study. Information about reef morphology and the location of each study were also recorded.

**Independency of experiments.** We defined each transect in the different reef environments as an “experiment”. Depending on the number and the position of sensors deployed on the reefs, we could identify more than one experiment for some of the published studies considered. To ensure independence between the experiments in cases where the studies were conducted on the same reef, but at different locations or times, we defined two transects as independent if they differed for at least one of the sensors by which they were delimited and if they could not be interpreted as one subset of the other (Fig. 1).

**Hedge’s  $g$  effect size.** All the analyses were also run using the Hedge’s  $g$ -effect size, another common effect size in meta-analysis, to evaluate the robustness of the results. Hedge’s  $g$  is based on the difference between treatment and control divided by their pooled standard deviation. To ensure comparability of studies when using this effect size, we based our analyses only on experiments

with the same measurement scale. In particular, when analyzing wave energy reduction, we only considered data available in ‘J m<sup>-2</sup>’ whereas for the wave height reduction analyses, we considered only data expressed in ‘m’. We therefore excluded data reported as ‘percentage’, which slightly decreased the sample size of some analyses in comparison to those based on the log response ratio. Results of the Hedge’s *g* analyses are provided in the Supplementary Fig. 4.

**Effects of incident wave energy and reef flat width on wave attenuation.** To investigate if wave attenuation was a function of the maximum incident wave energy or reef flat width, we fitted asymptotic regression models to the data and constrained the asymptote to be less than or equal to 100% reduction of wave energy and height.

When analyzing the relationship between the maximum incident wave energy and the corresponding wave energy reduction, we only used experiments where extracted data were available as a set of  $n$  paired observations [control ( $E_C$ ), treatment ( $E_T$ )] <sub>$i$</sub> ,  $1 \leq i \leq n$  with  $n > 1$ , and the unit measure was in J m<sup>-2</sup>. Therefore, it was possible to calculate percentage wave energy reduction associated to the maximum incident energy as  $100 - [(E_{Ti} / \max_{1 \leq i \leq n} E_{Ci}) \times 100]$ . Whenever the maximum value for incoming energy was shared between two or more paired observations for the same experiment, we conservatively selected the pair where the reduction in wave energy was the least. We constrained the regression model to start from the axes origin. The ranges of wave heights at the experiments’ control sites are reported in Supplementary table 2.

When analyzing the relationship between wave attenuation and reef flat width, we only used experiments where the distance between reef crest (control) and reef flat sensors (treatment) was known. For each experiment, percentage reduction for both wave energy and wave height were calculated as  $100 - [(\text{mean of treatment} / \text{mean of control}) \times 100]$ .

All analyses were done using R 2.11.1<sup>35</sup>.

**Conversion of coral restoration projects figures in \$ m<sup>-1</sup>.** We reported the costs of both breakwaters construction and coral reef restoration as adjusted 2012 US \$ using the on-line inflation converter available at [www.usinflationcalculator.com](http://www.usinflationcalculator.com). Costs provided in currency other than US \$ were converted to US \$ using the on-line [www.fxtop.com/en/currency-converter-past.php](http://www.fxtop.com/en/currency-converter-past.php) before to adjust for inflation.

**Spatial analysis of coral reefs and at risk coastal populations.** We used ArcGIS to extract all areas below 10 m elevation from the Global Digital Elevation Model (ETOPO2) provided by the National Geophysical Data Center (NGDC). We intersected the resulting raster of low-lying areas with the Global Rural-Urban Mapping Project (GRUMP) global population data set provided by the Center for International Earth Science Information Network (CIESIN), Columbia University. The resulting raster indicates total population residing in areas less than 10 m elevation.

We mapped coral reefs using the global data set provided by World Resources Institute, Reefs at Risk Revisited (2011). We applied two different buffers (10 km and 50 km) to the global reef data to identify all areas within the 10 km or 50 km zone of coral reefs. We then intersected these coral reef zones with the low-lying population raster data set to identify the number of people living below 10 m elevation and within 10 km or 50 km from reefs. Supplementary Fig. 5 is a detailed view of the Caribbean showing a portion of the coral reefs, 50 km zone, and low lying population raster used in our analysis. Using zonal statistics, we estimated the global and per country number of people in low-lying areas near reefs. Country zones were delineated by each country's land and maritime boundaries. Global country boundaries were provided by World Resources Institute, Reefs at Risk Revisited (2011) and maritime boundaries were provided by VLIZ (2011) Maritime Boundaries Geodatabase, version 6.1, Flanders Marine Institute.



**Supplementary Data 1. Experiments included in meta-analyses of wave energy reduction (WER).**

The information on the original publication (*author, year, title*) and on data used were reported for each experiment. *Data collection* indicates whether data were collected during a survey in the field (SURV), or resulted from experimental activity (EXP). *Original response variable* indicates the variable considered as cited in the original study ( $H_s$ = significant wave height;  $H_{rms}$ = root-mean-square wave height;  $H_{m0}$ = significant wave height). *Transformation* indicates whether the response variable used was a transformation of the original response variable (y/n). *Response variable used* and *variable unit*, indicate variable used in this study and its' unit measure ('E' is wave energy density calculated from  $H_{1/2}$  using equation (1) ). *Recovered data*, indicates the source of data within the paper. *Site, region*, refer to the geographical location of the reef studied. *Reef environment*, indicates which reef environment the experiment was evaluated (reef crest 'C', reef flat 'F', whole reef 'WR'). *Treatment sample size, treatment mean, treatment error, control sample size, control mean, control error, error*, are values used in the analyses. *Distance (m)* indicates the distance, in meters, between control and treatment as a proxy for reef flat width. *Effect size ( $\ln R$ )* is the log ratio effect size calculated by taking the natural logarithm of the ratio between the mean of treatment and mean of control. *Weighting factor ( $\ln R$ )* is the weighting factor associated with the log ratio effect size and calculated as the reciprocal of the variance under the random model. *Weighted effect size ( $\ln R$ )* is the log ratio weighted effect size calculated as the product *Effect size ( $\ln R$ )*  $\times$  *weighting factor ( $\ln R$ )*.

**Supplementary Data 2. Experiments included in meta-analyses of wave height reduction (WHR).**

Both information on the original publication (*author, year, title*) and on data used were reported for each experiment. *Data collection* indicates whether data were collected during a survey in the field (SURV), or resulted from experimental activity (EXP). *Original response variable* indicates the

variable considered as cited in the original study ( $H_s$ = significant wave height;  $H_{rms}$ = root-mean-square wave height;  $H_{m0}$ = significant wave height). *Transformation* indicates whether the response variable used was a transformation of the original response variable (y/n). *Response variable used* and *variable unit*, indicates the variable used in this study and its' unit measure. *Recovered data*, indicate the source of data within the paper. *Site, region*, refer to the geographical location of the reef studied. *Reef environment*, indicates which reef environment the experiment was evaluated (reef crest 'C', reef flat 'F', whole reef 'WR'). *Treatment sample size, treatment mean, treatment error, control sample size, control mean, control error, error*, are values used in the analyses. *Distance (m)* indicates the distance, in meters, between control and treatment as a proxy for reef flat width. *Effect size (ln R)* is the log ratio effect size calculated by taking the natural logarithm of the ratio between the mean of treatment and mean of control. *Weighting factor (ln R)* is the weighting factor associated with the log ratio effect size and calculated as the reciprocal of the variance under the random model. *Weighted effect size (ln R)* is the log ratio weighted effect size calculated as the product *Effect size (ln R) × weighting factor (ln R)*.

### **Supplementary Data 3. Experiments included in meta-analyses of wave energy reduction for different wave types.**

Both information on the original publication (*author, year, title*) and on data used were reported for each experiment. *Data collection* indicates whether data were collected during a survey in the field (SURV), or resulted from experimental activity (EXP). *Original response variable* indicates the variable considered as cited in the original study ( $H_s$ = significant wave height;  $H_{rms}$  = root-mean-square wave height;  $H_{m0}$ = significant wave height). *Transformation* indicates whether the response variable used was a transformation of the original response variable (y/n). *Response variable used* and *variable unit*, indicate variable used in this study and its' unit measure ('E' is wave energy density calculated from  $H_{1/3}$  using equation (1) ). *Recovered data*, indicate the source of data within the paper. *Site, region*, refer to the geographical location of the reef studied. *Reef environment*,

indicates which reef environment the experiment was evaluated (reef crest 'C', reef flat 'F'; F and C experiments were combined to analyze the effect of the whole reef 'WR'). *Wave type* indicates whether the study considered swell or wind waves. *Treatment sample size, treatment mean, treatment error, control sample size, control mean, control error, error*, are values used in the analyses. *Effect size (ln R)* is the log ratio effect size calculated by taking the natural logarithm of the ratio between the mean of treatment and mean of control. *Weighting factor (ln R)* is the weighting factor associated with the log ratio effect size and calculated as the reciprocal of the variance under the random model. *Weighted effect size (ln R)* is the log ratio weighted effect size calculated as the product  $Effect\ size\ (ln\ R) \times weighting\ factor\ (ln\ R)$ .

## Supplementary References

1. Falter, J.L., Atkinson, M.J. & Merrifield, M.A. Mass-transfer limitation of nutrient uptake by a wave-dominated reef flat community. *Limnology and Oceanography*. **49**, 1820-1831 (2004).
2. Storlazzi, C.D., Ogston, A.S., Bothner, M.H., Field, M.E. & Presto, M.K. Wave- and tidally-driven flow and sediment flux across a fringing coral reef: Southern Molokai, Hawaii. *Continental Shelf Research*. **24**, 1397-1419 (2004).
3. Lowe, R.J., Falter, J.L., Bandet, M.D., Pawlak, G., Atkinson, M.J., Monismith, S.G., *et al.* Spectral wave dissipation over a barrier reef. *J. Geophys. Res.* **110**, C04001 (2005).
4. Lowe, R.J., Falter, J.L., Monismith, S.G. & Atkinson, M.J. A numerical study of circulation in a coastal reef-lagoon system. *J. Geophys. Res.* **114**, C06022 (2009).
5. Lowe, R.J., Falter, J.L., Monismith, S.G. & Atkinson, M.J. Wave-driven circulation of a coastal reef-lagoon system. *Journal of Physical Oceanography*. **39**, 873-893 (2009).
6. Gourlay, M.R. Wave transformation on a coral-reef. *Coastal Engineering*. **23**, 17-42 (1994).
7. Hardy, T.A. & Young, I.R. Field study of wave attenuation on an offshore coral reef. *J. Geophys. Res.* **101**, 14311-14326 (1996).
8. Brander, R.W., Kench, P.S. & Hart, D. Spatial and temporal variations in wave characteristics across a reef platform, Warraber Island, Torres Strait, Australia. *Marine Geology*. **207**, 169-184 (2004).
9. Kench, P.S. & Brander, R.W. Wave processes on coral reef flats: implications for reef geomorphology using Australian case studies. *J. Coast. Res.* **22**, 209-223 (2006).
10. Jago, O.K., Kench, P.S. & Brander, R.W. Field observations of wave-driven water-level gradients across a coral reef flat. *J. Geophys. Res.* **112**, C06027 (2007).
11. Samosorn, B. & Woodroffe, C.D. Nearshore wave environments around a sandy cay on a platform reef, Torres Strait, Australia. *Continental Shelf Research*. **28**, 2257-2274 (2008).

12. Taebi, S., Lowe, R.J., Pattiaratchi, C.B., Ivey, G.N., Symonds, G. & Brinkman, R. Nearshore circulation in a tropical fringing reef system. *J. Geophys. Res.* **116**, C02016 (2011).
13. Péquignet, A.C., Becker, J., Merrifield, M. & Boc, S. The dissipation of wind wave energy across a fringing reef at Ipan, Guam. *Coral Reefs*. **30**, 71-82 (2011).
14. Lugo-Fernandez, A., Roberts, H.H. & Wiseman, W.J. Tide effects on wave attenuation and wave set-up on a Caribbean coral reef. *Estuar. Coast. Shelf. Sci.* **47**, 385-393 (1998).
15. Lugo-Fernandez, A., Roberts, H.H. & Suhayda, J.N. Wave transformations across a Caribbean fringing-barrier coral reef. *Continental Shelf Research*. **18**, 1099-1124 (1998).
16. Kench, P.S., Brander, R.W., Parnell, K.E. & O'Callaghan, J.M. Seasonal variations in wave characteristics around a coral reef island, South Maalhosmadulu atoll, Maldives. *Marine Geology*. **262**, 116-129 (2009).
17. Nakaza, E. & Hino, M. Bore-like surf beat in a reef zone caused by wave groups of incident short-period waves. *Fluid Dynamics Research*. **7**, 89-100 (1991).
18. Zhu, L.S., Li, M.Q., Zhang, H.S. & Sui, S.F. Wave attenuation and friction coefficient on the coral-reef flat. *China Ocean Engineering*. **18**, 129-136 (2004).
19. Blanchon, P., Iglesias-Prieto, R., Jordán Dahlgren, E. & Richards, S. Arrecifes de coral y cambio climático: vulnerabilidad de la zona costera del estado de Quintana Roo. In: Botello AV, Villanueva-Fragoso S, Gutiérrez J, Rojas Galaviz JL (eds). *Vulnerabilidad de las Zonas Costeras Mexicanas Ante el Cambio Climático*. (Universidad Autónoma de Campeche, Campeche, 229-248, 2010).
20. Pomeroy, A., Lowe, R., Symonds, G., Van Dongeren, A. & Moore, C. The dynamics of infragravity wave transformation over a fringing reef. *J. Geophys. Res.-Oceans*. **117**, 17 (2010).

21. Christianen, M.J.A., van Belzen, J., Herman, P.M.J., van Katwijk, M.M., Lamers, L.P.M., van Leent, P.J.M., *et al.* Low-canopy seagrass beds still provide important coastal protection services. *PLoS One*. **8**, e62413 (2013).
22. Ford, M.R., Becker, J.M. & Merrifield, M.A. Reef flat wave processes and excavation pits: observations and implications for majuro atoll, marshall islands. *J. Coast. Res.* **29**, 545-554 (2012).
23. Huang, Z.C., Lenain, L., Melville, W.K., Middleton, J.H., Reineman, B., Statom, N., *et al.* Dissipation of wave energy and turbulence in a shallow coral reef lagoon. *J. Geophys. Res.- Oceans*. **117**, 18 (2012).
24. Jeanson, M., Anthony, E.J., Dolique, F. & Aubry, A. Wave characteristics and morphological variations of pocket beaches in a coral reef-lagoon setting, Mayotte Island, Indian Ocean. *Geomorphology*. **182**, 190-209 (2013).
25. Mandlier, P.G. Field observations of wave refraction and propagation pathways on coral reef platforms. *Earth Surf. Process. Landf.* **38**, 913-925 (2013).
26. Filipot, J.F. & Cheung, K.F. Spectral wave modeling in fringing reef environments. *Coast. Eng.* **67**, 67-79 (2012).
27. Ogawa, H. Observation of wave transformation on a sloping type B shore platform under wind-wave and swell conditions. *Geo-Mar. Lett.* **33**, 1-11 (2013).
28. Shepard, C.C., Crain, C.M. & Beck, M.W. The protective role of coastal marshes: a systematic review and meta-analysis. *PLoS ONE*. **6**, e27374 (2011).
29. Gourlay, M.R. Wave set-up on coral reefs. 1. Set-up and wave-generated flow on an idealised two dimensional horizontal reef. *Coastal Engineering*. **27**, 161-193 (1996).
30. Gourlay, M.R. Wave set-up on coral reefs. 2. Set-up on reefs with various profiles. *Coastal Engineering*. **28**, 17-55 (1996).
31. Hozo, S., Djulbegovic, B. & Hozo, I. Estimating the mean and variance from the median, range, and the size of a sample. *BMC Med Res Methodol.* **5**, 13 (2005).

32. Holthuijsen, L.H. *Waves in oceanic and coastal waters*. (Cambridge University Press, Cambridge, UK, 404, 2007).
33. Herbers, T.H.C., Elgar, S. & Guza, R.T. Generation and propagation of infragravity waves. *J. Geophys. Res.* **100**, 24863-24872 (1995).
34. Bromirski, P.D., Sergienko, O.V. & MacAyeal, D.R. Transoceanic infragravity waves impacting Antarctic ice shelves. *Geophysical Research Letters*. **37**, L02502 (2010).
35. R Development Core Team. R: a language and environment for statistical computing. (R Foundation for Statistical Computing, Vienna, Austria, 2012). Available from: [www.r-project.org](http://www.r-project.org)